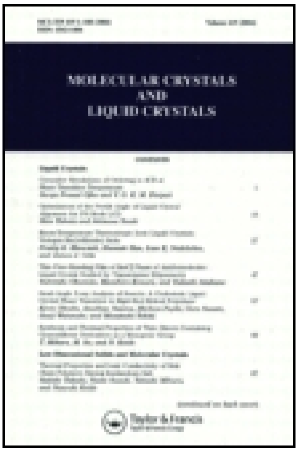
MOLECULAR CRYSTALS AND LIQUID CRYSTALS

Molecular Crystals and Liquid Crystals
Publication details, including instructions for authors and subscription information:
http://www.tandfonline.com/loi/gmcl20

Characteristics of Facing Target-Sputtered Amorphous InGaZnO Thin Films as the Active Channel Layer in Transparent Thin Film Transistor on Polymeric Substrate

Han Jae Shin [a], Dong Cheul Han [a], Young Cheol Choi [a] & Do Kyung Lee [a]

[a] Mobile Display Research Center, Gumi Electronics and Information Technology Research Institute, Gumi, Gyeongsangbuk-do, 730-853, Korea

Version of record first published: 18 Oct 2011

Mol. Cryst. Liq. Cryst., Vol. 550: pp. 13–22, 2011

ISSN: 1542-1406 print/1563-5287 online
DOI: 10.1080/15421406.2011.600180

Characteristics of Facing Target-Sputtered Amorphous InGaZnO Thin Films as the Active Channel Layer in Transparent Thin Film Transistor on Polymeric Substrate

HAN JAE SHIN, DONG CHEUL HAN, YOUNG CHEOL CHOI, AND DO KYUNG LEE*

Mobile Display Research Center, Gumi Electronics and Information Technology Research Institute, Gumi, Gyeongsangbuk-do, 730-853, Korea

For an application to the channel layer in flexible transparent thin-film transistor (TFT), we have prepared the amorphous indium gallium zinc oxide (a-InGaZnO) thin films on unheated polyethylene naphthalate (PEN) substrate by facing target sputtering. Two types of a-InGaZnO TFT design, one top gate configuration and the other bottom gate, have been fabricated for comparison with each other. The experimental results reveal that the top gate a-InGaZnO TFT is shown to be superior TFT performances, compared with bottom-gate structure. As a result, the top gate a-InGaZnO TFTs operate in depletion mode with a threshold voltage of −0.5 V, a mobility of 6.0 cm^2/Vs, an on-off ratio of $>10^6$, and a sub-threshold slope of 0.95 V/decade. In addition, the optical transmittance of about 74% at 550nm wavelength is represented for the top gate a-InGaZnO TFT on PEN.

Keywords Facing Target Sputtering; Amorphous InGaZnO Thin Films; Active Channel Layer; Flexible Transparent Thin Film Transistors

Introduction

Since Nomura et al. reported the fabrication of amorphous indium gallium zinc oxide (a-InGaZnO)-based thin film transistors (TFTs) with high performance [1], they have attracted much attention due to high mobility, good uniformity and low processing temperature [2–5]. In the a-IGZO-based TFTs, the channel layer grown at low temperatures allows the use of plastic substrates for the realization of flexible and transparent displays. Recently, the a-InGaZnO thin film as an active channel layer has been reported to the successful deposition by conventional magnetron sputtering method [6]. This technique generally provides such benefits as high deposition rates, uniformity over the large area, and low processing temperatures [7], which has been used extensively in the industrial mass production.

However, in spite of above merits, the problem of conventional magnetron sputtering method has the unwanted bombardments of the growing channel film by negative ions and high energy neutral atoms in the plasma, which results in low TFT performances due to the increase in the surface morphology roughness of the channel. Also, in the film deposition

*Corresponding author. E-mail: dklee@geri.re.kr

on polymeric substrate, it is not easy to avoid plasma damage on the substrate, resulting in the cracks or rough surface of the film.

To overcome these problems, the damage-free deposition at low temperature is necessary to the reduction in the film stress and smooth surface of the film [8]. A facing target sputtering (FTS) method [9] can be regarded to be useful to realize the deposition of a-InGaZnO films with high quality because the bombardments of high energy oxygen atoms and secondary electrons are dramatically suppressed during the deposition.

Thus, this paper presents characteristics of the a-InGaZnO-based TFTs on polyethylene naphthalate (PEN) substrate fabricated by using the FTS system. In particular, electrical performances of a-InGaZnO TFTs are mainly investigated with respect to TFT design.

Experimentals

The a-InGaZnO thin films were prepared by the FTS method on the PEN (Teijin Dupont Films) substrate at room temperature, varying injection power to the sputter guns. Prior to deposition, PEN substrates were cleaned with acetone, methanol and de-ionized water for 10 min in an ultrasonic bath. The base pressure in the chamber was adjusted to 1.0×10^{-6} Torr and the pressure during the deposition was maintained at 3 mTorr. The composition ratio of dual rectangular targets used in the experiment was In_2O_3: Ga_2O_3: ZnO = 1: 1: 1 in molar percentage with purity of 99.99%.

The thickness of the a-InGaZnO thin films was determined by a surface profiler (KLA Tencor, Alpha-Step IQ). In order to examine the crystallinity of the films, x-ray diffraction (Rigaku, D/MAX-2500) measurement was performed. X-ray diffraction patterns did not contain any peaks attributable to crystals, showing amorphous nature. The electrical properties of a-InGaZnO thin films were measured by the Hall Effect measurement (Ecopia, HMS-3000). The surface morphology of the films was monitored by atomic force microscopy (AFM) (Park Systems Corp., XE-100). Optical transmittance characteristics of the films and TFT devices were measured by means of an ultraviolet-visible spectrophotometer (Otsuka, MCPD-7000) in the visible region.

The schematic cross-sections of the fabricated a-InGaZnO TFTs with top gate and bottom gate configurations are shown in Figure 1. For serving gate, source and drain electrodes, transparent conducting indium zinc tin oxide (IZTO) thin films, which is the 7 wt% Zn and 3 wt% Sn co-doped In_2O_3 electrodes, were deposited to a thickness of 200 nm by conventional magnetron sputtering. A SiO_2 gate dielectric with the thickness of 100 nm was deposited by electron beam evaporation. The a-InGaZnO channel layer was deposited to 50 nm thickness using FTS method. In the fabrication of top gate a-InGaZnO TFT, source and drain electrodes were defined by photolithography and wet-etching technique. The other was defined by photolithography and lift-off technique. In the bottom gate configuration, all layers except gate electrode were defined by photolithography and lift-off technique. Concerning the electrical characterization for the a-InGaZnO-based TFTs, it was used a probe station and a semiconductor parameter analyzer (Agilent E5270B).

Results and Discussion

Figure 2 indicates the influence of injection power on the electrical properties of a-InGaZnO thin films deposited on PEN substrate. The resistivity of the films decreases with injection power up to 140 W, while the resistivity increases at 150 W. This may be due to the re-sputtering of high energetic sputtered ions and atoms on PEN. It is worth noting that

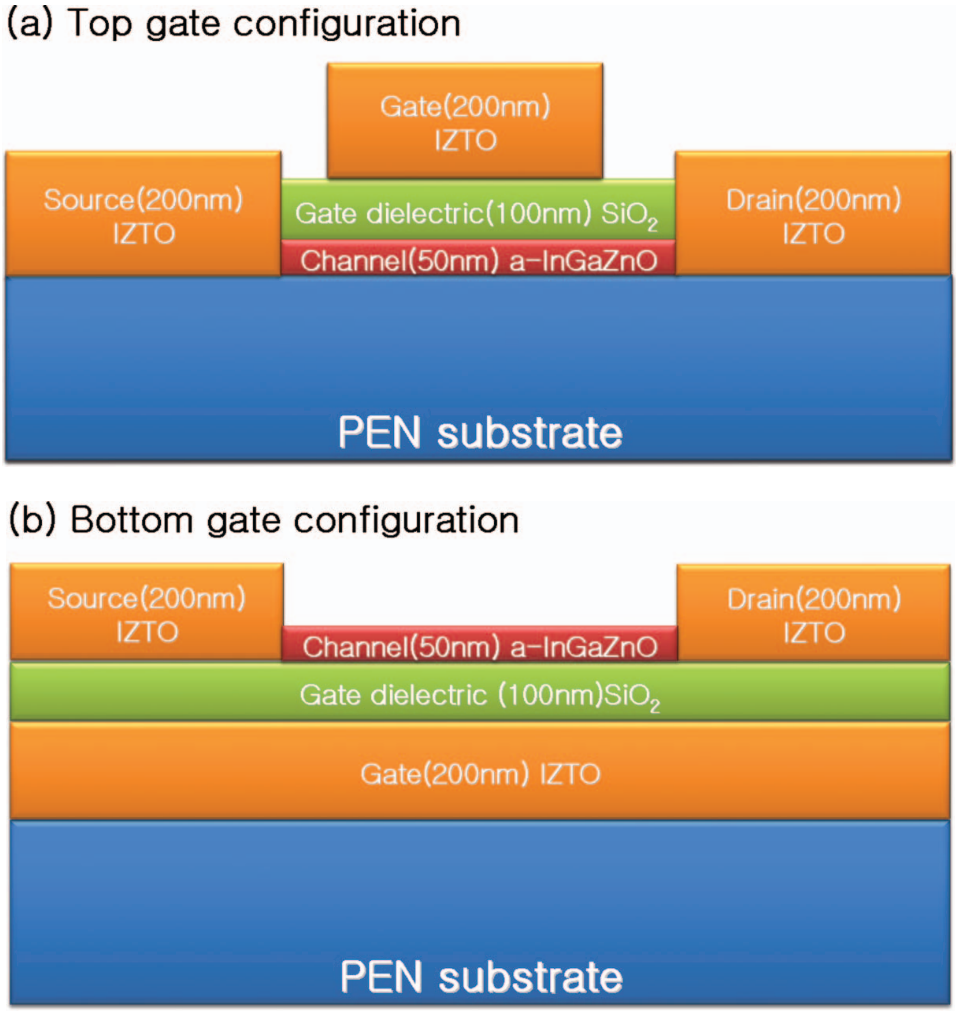

Figure 1. Cross-sectional diagrams of a-InGaZnO-based TFT.

the a-InGaZnO films deposited at 120 W shows the resistivity of about 6.1 Ωcm, which is within the range of resistivity for usable semiconductor in the oxide TFT [10]. It is also known that in the oxide TFTs, the channel layer must be fabricated with low carrier concentration and high mobility [11]. Accordingly, the a-InGaZnO film grown at 120 W serves well as the active channel layer in the transparent TFT applications, showing the carrier concentration of about 6.5×10^{16} /cm^3 and Hall mobility of about 15.6 cm^2/Vs. From this result, we have decided that the a-InGaZnO thin film deposited at injection power of 120 W is applied to the channel active layer in the flexible transparent TFT devices, and the subsequent investigation on characteristics of a-InGaZnO TFTs is conducted.

Figure 3 shows the AFM images of the active channel in the a-InGaZnO TFTs. With a viewpoint of top gate configuration, the a-InGaZnO channel layer on PEN has a surface uniformity with a root mean square value (RMS) of roughness of about 1.77 nm. On the other hand, the a-InGaZnO layer on SiO_2/IZTO/PEN substrate, which corresponds to

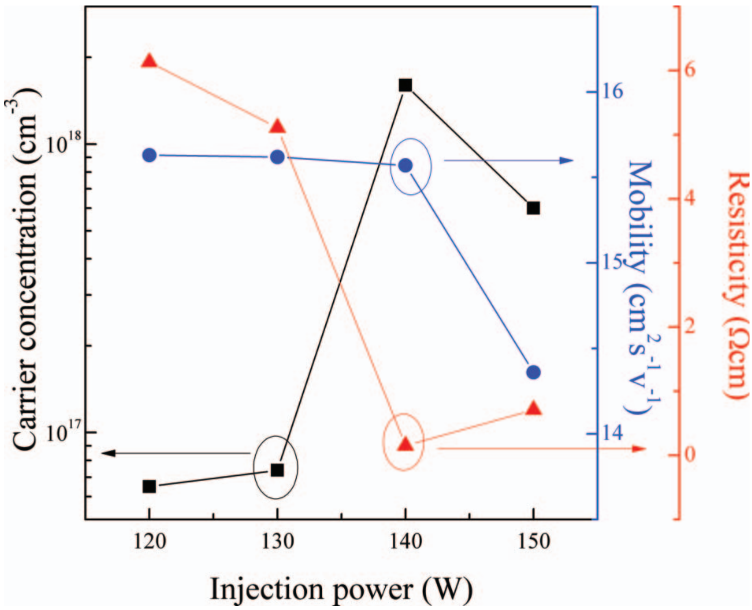

Figure 2. Effect of injection power on the electrical properties of a-InGaZnO thin films on PEN substrate.

the bottom gate structure, has a RMS roughness of about 4.12 nm. This means that the active channel within the top gate a-InGaZnO TFT relatively has the smoother surface morphology. The smooth surface morphologies of the a-InGaZnO thin films can develop good interfaces for the regions between electrodes and the active channel [12].

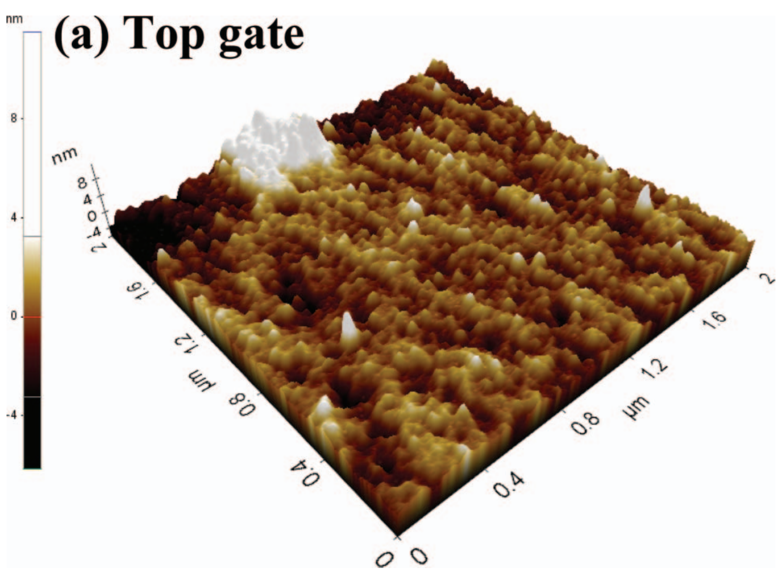

Figure 3. AFM images of a-InGaZnO thin films. *(Continued)*

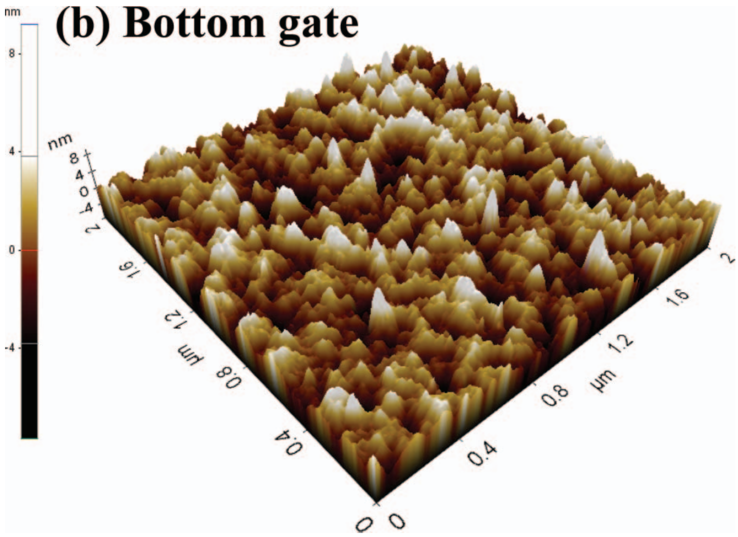

Figure 3. (Continued)

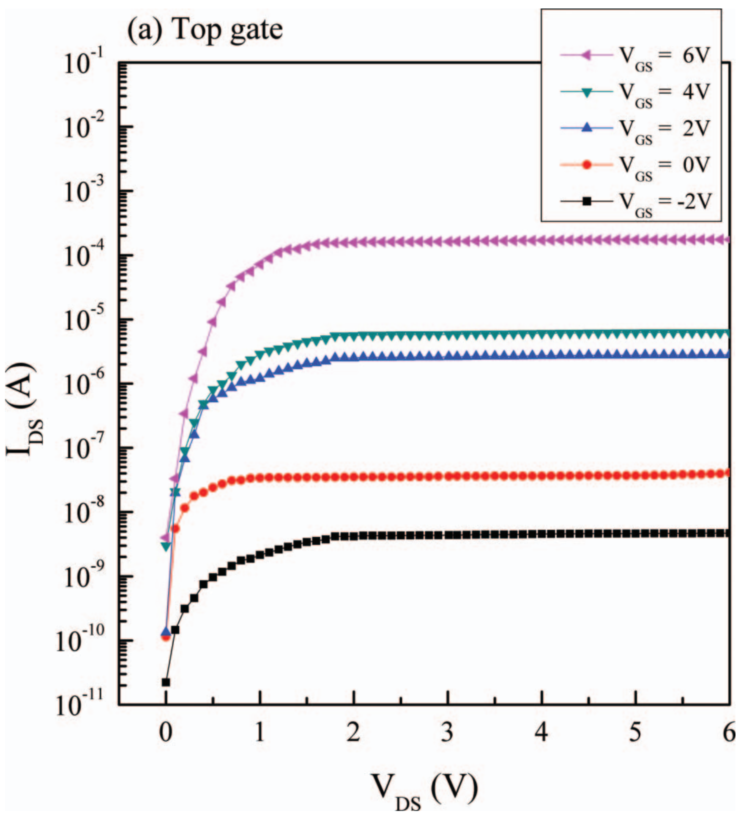

Figure 4. The output characteristics of a-InGaZnO-based TFTs. *(Continued)*

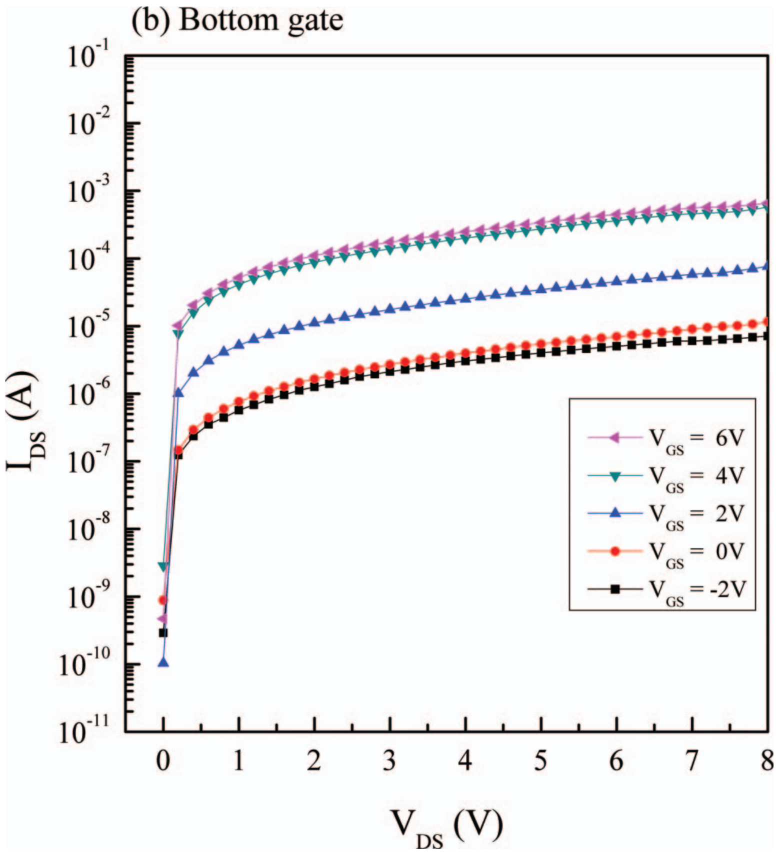

Figure 4. (Continued)

The output characteristics of a-InGaZnO-based TFTs are illustrated in Figure 4. It is found that the drain to source current (I_{DS})—the drain to source voltage (V_{DS}) curves for both TFTs have appreciable I_{DS} at zero gate bias (V_{GS}) and the TFTs do not turn off without the application of negative V_{GS}, indicating that the devices operate in depletion mode. From the figures, it is also found that a-InGaZnO TFT with top gate design exhibits relatively excellent hard saturations from the fact of flatness for the I_{DS} curves for high V_{DS}. In addition, under the same operation conditions, top gate a-InGaZnO TFT shows less irregular separation between I_{DS} in saturated region, compared to the bottom gate TFT. Theses results may be originated in the mobility effect associated with interface roughness scattering, resulting from the differences of device configuration and fabrication procedure. Specifically, from the AFM result, the RMS roughness value of a-InGaZnO film within top gate structure is lower than that of the film within the bottom gate, as mentioned above. The smooth surface morphology leads to a good interface between the source/drain electrodes and the channel layers. Good interface can ensure a reduced role of interface states on carrier transport across the drain and source [13], resulting in the increasing field-effect mobility. Also, in the fabrication procedure of bottom-gate a-InGaZnO TFT, the surface of SiO_2 gate dielectric layer has been exposed to multiple processing before the a-InGaZnO channel layer deposition, which may roughen the channel-dielectric interface. Hence, the

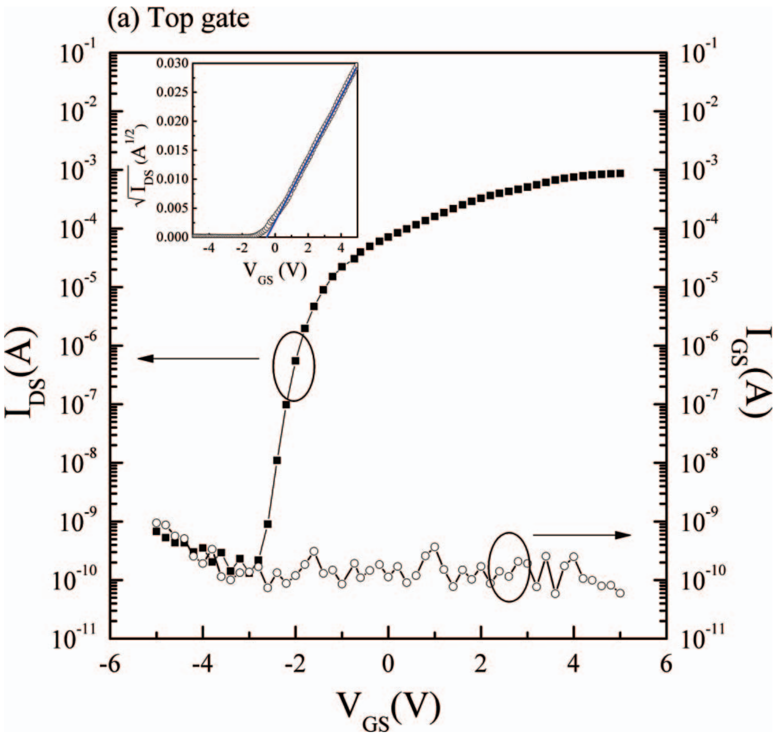

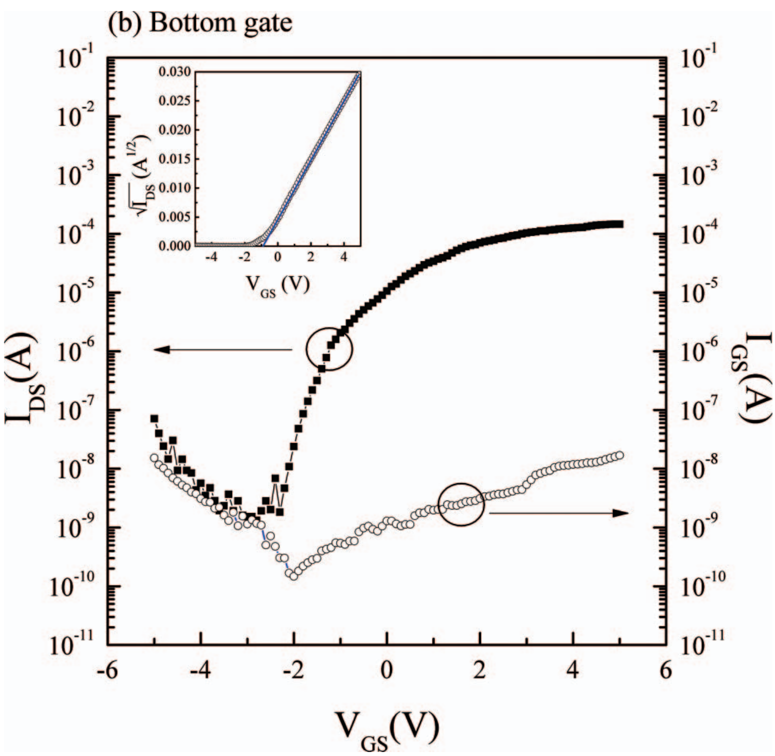

Figure 5. The transfer characteristics and gate leakage current of a-InGaZnO-based TFTs. The respective inserted figures are the plots of square root of I_{DS} vs V_{GS} in the corresponding figure.

mobility degradation related with the increase of interface roughness scattering [14, 15] may be occurred in the bottom gate a-InGaZnO TFT.

Figure 5 shows the transfer characteristics and gate leakage current (I_{GS}) for a-InGaZnO TFTs with a W/L ratio of 10 for $V_{DS} = 6$ V. Both a-InGaZnO TFTs represent the n-channel characteristics because electrons are generated by low negative V_{GS}. As shown in Figure 5, the respective off-currents less than 10^{-9} and 10^{-7} A are observed for top gate and bottom gate a-InGaZnO TFTs. All I_{DS} are increased by the positive V_{GS} and reach to 10^{-3} A order. The I_{GS} of a-InGaZnO TFTs with top gate and bottom gate structure are measured to be $10^{-9}\sim10^{-10}$ A and $10^{-7}\sim10^{-10}$ A, respectively. The respective on/off current ratio for operation in the saturation region is estimated to be about $>10^6$ and 10^5 for top gate and bottom gate a-InGaZnO TFTs. The sub-threshold characteristics of the a-InGaZnO TFTs describe the operation of the TFT at gate voltages lower than threshold voltage (V_{TH}). From the transfer characteristics, the sub-threshold slope is defined as

$$S = \frac{dV_{GS}}{d(\log I_{DS})}$$

and can be found from the inverse slope of the curves in Figure 5. We obtain the values of about 0.95 and 0.9 V/decade, respectively, for the top gate and the bottom gate a-InGaZnO TFT. The field-effect mobility (μ_{FE}) and the threshold voltage (V_{TH}) can be calculated by the fitting a straight line to the plot of square root of I_{DS} vs V_{GS} [16, 17], as shown in the inserted figures in Figure 5, according to the expression

$$I_{DS} = \left(\frac{C_i \mu_{FE} W}{2L}\right)(V_{GL} - V_{TH})^2 \qquad \text{for } V_{DS} > V_{GS} - V_{TH},$$

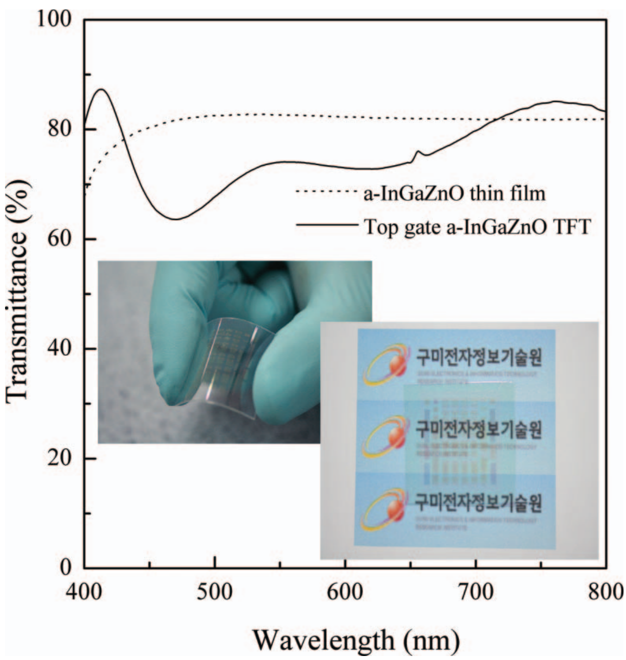

Figure 6. The optical transmittances of a-InGaZnO thin film and top gate a-InGaZnO TFT on PEN substrate. The inserted is the photographs of the fabricated a-InGaZnO TFT.

where C_i is the capacitance per unit area of the gate insulator. An a-InGaZnO TFT with bottom gate configuration exhibits a μ_{FE} of 0.52 cm^2/Vs and a V_{TH} of -0.9 V, whereas the top gate a-InGaZnO TFT shows the μ_{FE} of 6.0 cm^2/Vs and the V_{TH} of -0.5 V. The μ_{FE} is well known to be the most important TFT electrical parameter, because it quantifies the semiconductor channel layer performance with standpoints of current device capability and maximum switching frequency. Compared to bottom gate a-InGaZnO TFT, the higher μ_{FE} of the top gate a-InGaZnO TFT may be attributed by the smaller interface roughness scattering, as described in the explanation for Figure 4, due to smooth surface morphology of the channel.

Figure 6 shows the optical transmittances of a-InGaZnO thin film and top gate a-InGaZnO TFT on PEN substrates in the wavelength range between 400 and 800nm. The average transmittance of a-InGaZnO thin film including the PEN substrate at 550 nm wavelength is observed to be about 82.6%. It is also found that the average optical transmission of the a-InGaZnO TFT at 550 nm is about 74%, which indicates good characteristics of transparent TFT. The inserted photographs indicate the fabricated a-InGaZnO TFT in this study, showing that the underlying text is visible.

Conclusions

In summary, a-InGaZnO thin films have been prepared by a facing target sputtering method at room temperature. We have performed the fabrication and characterization of a-InGaZnO TFTs on the PEN substrate with respect to the TFT structure design. Our experimental results reveal that the TFT performance of a-InGaZnO TFT with top gate is superior to that of the bottom gate. The electrical performance of the top gate a-InGaZnO TFT device exhibits the field-effect of 6.0 cm^2/Vs, the on/off ratio of about $>10^6$ and the sub-threshold slope of 0.95 V/decade. Additionally, the optical transmittance of the top gate a-InGaZnO TFT on PEN at 550nm wavelength is about 74%. Therefore, this study suggests that the deposition by facing target sputtering can be an excellent fabrication method for the channel layer in the flexible transparent TFT with top gate configuration.

References

[1] Nomura, K., Ohta, H., Takagi, A., Kamiya, T., Hirano, M., & Hosono, H. (2004). *Nature*, 432, 488.

[2] Chiang, H. Q., McFarlane, B. R., Hong, D., Presley, R. E., & Wager, J. F. (2008). *J. Non-Cryst. Solid.*, **354**, 2826.

[3] Tsao, S. W., Chang, T. C., Huang, S. Y., Chen, M. C., Chen, S. C., Tsai, C. T., Kuo, Y. J., Chen, Y. C., & Wu, W. C. (2010). *Solid-State Electron*, **54**, 1497.

[4] Lim, W., Douglas, E. A., Norton, D. P., Pearton, S. J., Ren, F., Heo, -Y. -W., Son, -S. -Y., & Yuh, -J. -H. (2010). *Appl. Phys. Lett.*, **96**, 053510.

[5] Lee, -J. -S., Park, -J. -S., Pyo, -Y. -S., Lee, -D. -B., Kim, -E. -H., Stryakhilev, D., Kim, -T. -W., Jin, -D. -U., & Mo, -Y. -G. (2009). *Appl. Phys. Lett.*, **95**, 123502.

[6] Ito, M., Kon, M., Ishizaki, M., & Sekine, N. (2005). *Proc. IDW-AD'05*, p. 845.

[7] Lin, S., Chen, Y., Wang, C., Kao, K., & Chan, C. (2009). *J. Electr. Mater.*, **38**, 453, 17.

[8] Diallo, K., Erouel, M., & Tardy, J. (2007). *Appl. Phys. Lett.*, **91**, 183508.

[9] Tominaga, K., Yasuda, T., Kume, M., &Tada, O. (1985). *Jpn. J. Appl. Phys.*, **24**, 944.

[10] Fortunato, E., Barquinha, P., Goncalves, G., Pereira, L., & Martins, R. (2008). *Solid-State Electron*, **52**, 443.

[11] Yamada, T., Ikeda, K., Kishimoto, S., Makino, H., & Yamamoto, T. (2006). *Surf. Coat. Tech.*, **201**, 4004.

[12] Kwon, -J., Seo, -J., Shin, -S., & Ju, -B. -K. (2009). *J. Phys. D: Appl. Phys.*, **42**, 065105.
[13] Dhananjay, Cheng, S. S., Yang, C. Y., Ou, C. W., Chuang, Y. C., Wu, M. C., & Chu, C. W. (2008). *J Phys D: Appl Phys*., **41**, 092006.
[14] Yamanaka, T., Fang, S. J., Lin, H. C., Snyder, J. P., & Helms, C. R. (1996). *IEEE Electron Device Lett*., **17**, 178.
[15] Fritz, S. E., Kelley, T. W., & Frisble, C. D. (2005). *J. Phys. Chem.*, **B109**, 10574.
[16] Schroder, D. K. (1998). *Semiconductor Material and Device Characterization*, Wiley: New York.
[17] Hoffman, R. N. (2004). *J. Appl. Phys.*, **95**, 5813.